Electron capture from Li(2s) by doubly charged ions (5—40 keV)

F. Aumayr, G. Lakits, and H. Winter
Institut für Allgemeine Physik, Technische Universität Wien, Karlsplatz 13, A-1040 Wien, Austria
(Received 22 July 1985)

Total single-electron-capture cross sections have been measured for impact of N^{2+}, Ne^{2+}, Ar^{2+}, Kr^{2+}, and Xe^{2+} at 5—40 keV on Li(2s). The results are compared with other available data and can be quantitatively explained with a modified classical over-barrier transition model, assuming primary-ion-core conservation and taking into account the respective arrangements of available final projectile states.

I. INTRODUCTION

Electron capture is an important balance process in hot plasmas which contain both multicharged ions and neutral particles. In recent years, corresponding atomic collision experiments have gradually converged toward the simplest conceivable collision systems, which are composed of fully stripped ions and atomic hydrogen. For such systems the understanding of electron-capture processes is now fairly detailed, because also elaborate quantum-mechanical calculations have been carried out for comparison (for a recent review of the field, cf. Ref. 1). At low impact energies ($E < 25$ keV/amu), electron capture from alkali atoms by multicharged ions is of comparable simplicity, because the relatively small binding energy of the outermost alkali electron assures a quasi-one-electron character of the collision systems. This is especially true for capture from Li(2s), for which pronounced final-state selectivity has been found, in agreement with the quasi-one-electron behavior.[2,3] Such state-selective informations are of great interest for Li beam-activated charge-exchange spectroscopy, which represents an advanced diagnostic method for impurity-ion—transport studies in magnetically confined fusion plasmas.[4]

In the present work we deal with single-electron capture from Li(2s) by N^{2+}, Ne^{2+}, Ar^{2+}, Kr^{2+}, and Xe^{2+}, respectively. In this way we link previous studies on electron capture from Li(2s) by singly charged ions[5–9] with similar ones for multicharged ions.[2,3,10,11] Total capture cross sections for doubly charged projectiles have so far only been measured for He^{2+},[12] and at relatively low impact energies for the heavier noble gas ions.[11] Related state-selective measurements have been carried out for He^{2+},[13] and in less detail for C^{2+}, N^{2+},[2] and Ne^{2+}.[14]

Our data are compared with results from the above-cited studies, as well as with predictions from the classical over-barrier transition model (CBM, Refs. 15 and 16). The CBM is generally applicable and rather simple, and has worked remarkably well for capture by multicharged ions from Li(2s),[3] both in respect to total capture cross section and population of most probable final states.

II. EXPERIMENTAL METHOD, DATA EVALUATION, AND RESULTS

The measurements have been performed with a slightly modified version of the setup described in Ref. 7; see Fig. 1. Beams of doubly charged ions were obtained from an ion accelerator with a Duoplasmatron source and analyzer magnet, cleaned from charge-exchanged species by means of two parallel-plate condensers and passed through a Li vapor-filled target cell. The latter could be removed out of the ion-beam path to correct for electron capture from background-gas molecules. The background-gas pressure in the collision region was kept below 5×10^{-7} mbar. Immediately behind the collision cell the original doubly charged ions could be separated from charge-exchanged particles by means of a parallel-plate condenser field with a shielded Faraday cup (FC1) serving for ion-current measurement.

Figure 2 shows a typical course of ion current versus deflection voltage U_d across the condenser plates. One can clearly distinguish two plateau regions, the first (current I_A) corresponding to a mixture of doubly charged and singly charged ions, and the second (current I_B) due to singly charged ions produced by electron capture. For still higher values of U_d, only a neutral component could reach FC1. Its corresponding particle flux J_0 was determined via secondary-electron emission within FC1 by separating the electrodes of the latter as described

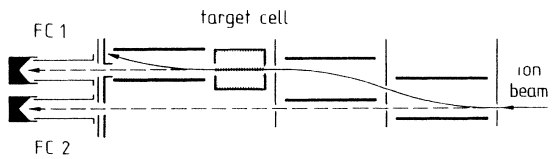

FIG. 1. Sketch of experimental setup with two parallel-plate condenser fields for ion-beam cleaning, Li-vapor target cell, charge-state-separation field, and Faraday cups. FC2 served for monitoring primary-ion-beam stability.

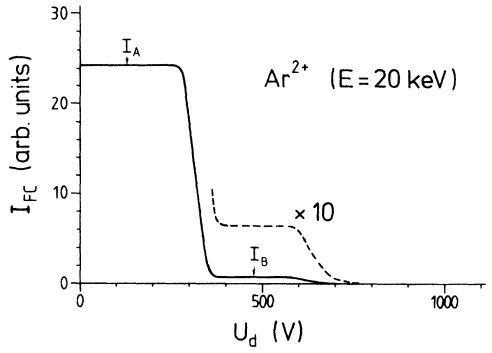

FIG. 2. Typical characteristics for ion-beam current measured in FC 1 vs deflection voltage U_d of separation field.

in Ref. 7. By proper choice of all beam apertures and the opening of FC1 as well as the length of the deflection field, the formation of well-established current plateaus was possible for all primary ion energies between 5 and 40 keV.

The particle fluxes J_q corresponding to doubly and singly charged ions ($q=2$ and 1, respectively) were derived from the ion currents

$$J_1=I_B/e,\quad J_2=(I_A-I_B)/2e\ . \tag{1}$$

Fractions of particles with charge state q ($q=0$, 1, or 2) in the post-collision ion beam are given by

$$F_q=J_q\Big/\sum_n J_n,\quad n=0,1,2\ . \tag{2}$$

With the assumptions (a) $F_2\gg F_1\gg F_0$ ("single-collision conditions") and (b) $\sigma_{20},\sigma_{01},\sigma_{12}\ll\sigma_{21}$ (negligible cross sections for double-electron capture and stripping), we can calculate the fractions F_q for a beam of doubly charged ions having passed through a Li target with thickness Π,

$$\begin{aligned}F_2&=\exp(-\sigma_{21}\Pi)\ ,\\ F_1&=\frac{\sigma_{21}}{\sigma_{21}-\sigma_{10}}[\exp(-\sigma_{10}\Pi)-\exp(-\sigma_{21}\Pi)]\ ,\\ F_0&=\frac{1}{\sigma_{21}-\sigma_{10}}[\sigma_{10}\exp(-\sigma_{21}\Pi)-\sigma_{21}\exp(-\sigma_{10}\Pi)]+1\ .\end{aligned} \tag{3}$$

Condition (a) was taken care of by keeping to a sufficiently small value of Π, which was also varied for checking a linear dependence of measured cross sections on target thickness. Condition (b) holds very well in the present impact-energy range for electron capture from Li(2s) by doubly charged ions. Cross sections σ_{10} for the corresponding singly charged ions have been measured up to 20 keV and, for the purpose of the present study, could be reliably extrapolated up to $E=40$ keV.[17] The target thickness Π was determined by calibration to our previously measured electron-capture cross sections for H^+-Li(2s) impact at 10 keV.[7,8] For this purpose, during the measurements frequent switchings were made between the doubly charged ion beam under study and a proton beam, with the target thickness remaining essentially constant.

With these data the cross sections σ_{21} could be deduced from currents I_A, I_B, the neutral particle flux J_0, and Eqs. (1)—(3). Corresponding results are given in Table I and Figs. 3(a) and 3(b). Data from repeated measurements usually coincided within 5%. The systematic errors were dominated from the target thickness (experimental error ±20%). Both the statistical and total errors are given in Table I. The statistical error was never larger than indicated by the size of symbols in Figs. 3(a) and 3(b).

For all beams of doubly charged ions, non-negligible metastable fractions have been present, the amount of which depended on the ion-source-discharge conditions.[18] A further discussion of this fact and its consequences will be given in Sec. III C.

III. DISCUSSION OF RESULTS

A. Comparison with available data

For Ne^{2+} our results are in full agreement with measurements of Waggoner *et al.*,[11] which partially overlap with our region of impact energies, cf. Fig. 3(a). The data of Rille and Winter[14] for impact energies from 20 to 60 keV have been obtained by another method as used by us, and are by a factor of 2—2.5 larger than our corresponding cross sections. The disagreement exceeds by far the combined error limits, and we conclude that the data of

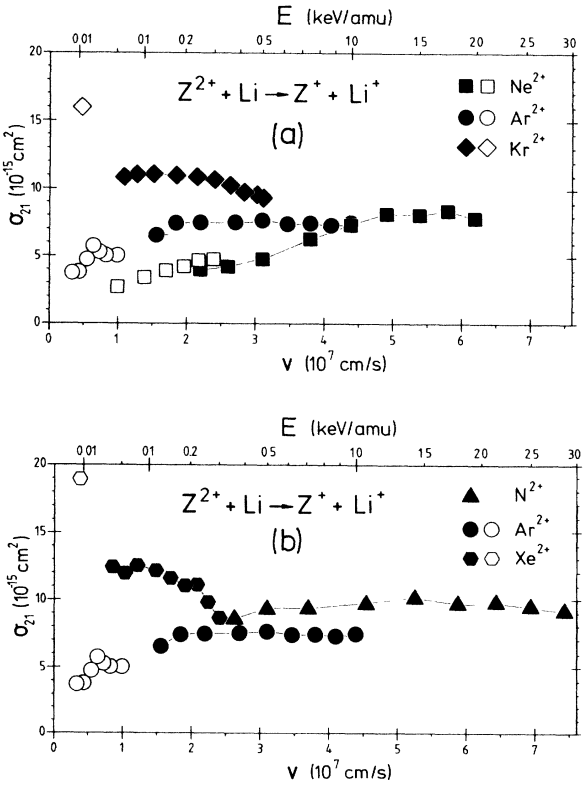

FIG. 3. (a) Total single-electron-capture cross sections for impact of Ne^{2+}, Ar^{2+}, and Kr^{2+} on Li(2s). Solid symbols: present measurements. Open symbols: data from Ref. 11. (b) Same as (a) for N^{2+}, Ar^{2+}, and Xe^{2+}. Ar^{2+} data have been plotted in both figures for comparison with other cross sections.

TABLE I. Measured total cross sections for single-electron capture by some doubly charged ions from Li($2s$) atoms. E denotes primary ion impact energy.

	σ_{21} (10^{-15} cm^2)					Statistical	Total
E (keV)	N	Ne	Ar	Kr	Xe	error (±%)	error (±%)
5	8.7	4.0	6.5	10.9	12.5	8	23
7	9.3	4.1	7.4	11.0	12.0	6	22
10	9.4	4.7	7.5	11.1	12.6	4	21
15	9.7	6.2	7.5	11.0	12.2	4	21
20	10.2	7.3	7.7	10.8	11.6	4	21
25	9.6	8.2	7.4	10.8	11.0	4	21
30	9.8	8.1	7.4	10.3	11.1	4	21
35	9.4	8.4	7.3	9.8	9.8	4	21
40	9.1	7.8	7.4	9.6	8.6	4	21

Ref. 14 are probably in error.

For Ar^{2+}, our cross sections are also in agreement with data from Ref. 11, besides the nonoverlapping impact-energy regions, cf. Figs. 3(a) and 3(b). Both for Kr^{2+} and Xe^{2+}, in Ref. 11 only a single cross section at 1 keV has been given. In comparison with our values for impact energies of ≥ 5 keV, especially for Xe^{2+}, there seems to be some disagreement, unless there is no (unexpectable) sudden jump of the respective σ_{21} between 1 and 5 keV. Finally, for N^{2+} no other data for comparison are known to us.

B. Impact-energy dependence

It is now well known that total electron-capture cross sections only depend strongly on impact energy, if a small number of states participates in the electronic transitions connected with the capture process. For all species investigated, we found no marked structure in the impact-energy characteristics, which points to a relatively large number of states taking part in the capture. For Ne^{2+} and Ar^{2+}, cross section σ_{21} rises with E up to a flat region, whereas for Kr^{2+} and Xe^{2+} the opposite behavior is found. For N^{2+} the cross sections remain more or less constant. Some qualitative explanations for these properties will be given in Sec. III D.

C. Comparison with classical over-barrier transition model

In the given impact-energy region, electron capture from Li($2s$) by multicharged ions can be regarded as a one-electron transition. For such cases a classical description of the electronic transitions over the potential barrier between the colliding particles is justified and should deliver realistic values of the total capture cross sections.

The classical over-barrier transition model (CBM) assumes a continuous distribution of the final projectile states. It was set up for an atomic-hydrogen target by Ryufuku *et al.*[15] and generalized for arbitrary target atoms.[16] Within the CBM description, an electron can pass over the potential barrier from the target atom (initial binding energy I_t) into the projectile Z^{q+}, which is regarded as a point charge q, at a distance $R \leq R_c$ with

$$R_c/a_0 = (2q^{1/2}+1)/[I_t/(1\text{ a.u.})] . \quad (4)$$

For doubly charged ions Z^{2+} and Li($2s$) target atoms we get $R_c = 10.2$ Å. If capture into a given final state $Z^+(n,l)$ corresponds to a reaction energy defect ΔE, resonance of binding energies for initial and final states occurs at a distance R,

$$R/a_0 = 1/[\Delta E/(1\text{ a.u.})] , \quad (5)$$

because of the long-range Coulomb interaction between reaction products.

In Fig. 4 we give diagrams of projectile final states corresponding to electron capture from Li($2s$) by Ne^{2+}, Ar^{2+}, and Xe^{2+}, respectively. For these diagrams we have assumed that all the ion states present in the primary ion beam (i.e., ground state as well as metastable Z^{2+}) remain unchanged during capture ("core conservation"—CC).

It has been demonstrated by experiment that, for capture from Li($2s$) by C^{2+} or N^{2+}, CC is given.[2] Recently, the same behavior was also found for singly charged projectiles.[17] Therefore, we can also assume CC for doubly charged noble-gas ions. Consequently, a variable metastable ion-beam fraction can be of no marked influence on the σ_{21} values, because capture into either primary ion species populates final states with very similar patterns of binding energies, cf. Fig. 4. The dashed line in Fig. 4 indicates a binding-energy resonance at $R=\infty$ ($\Delta E=0$), while the dotted line marks a binding-energy resonance at $R=R_c$.

For Ne^{2+}, Fig. 4 shows no resonant Ne II states available at R_c. Therefore, in this collision system electron capture becomes only possible at considerably smaller internuclear distances. The CBM predicts a cross section

$$\sigma_{21}^{\text{CBM}} = \frac{\pi}{2}R_c^2 = 16.3\times10^{-15}\text{ cm}^2 ,$$

which should be an absolute upper limit within the classical description.

All our σ_{21} data shown in Figs. 3(a) and 3(b) obey this limit. The same is true for capture by He^{2+} from Li($2s$), for which a maximum σ_{21} of 13.1×10^{-15} cm^2 at $E=0.65$ keV/amu has been measured by Dijkkamp *et al.*[13] Considering the actually available final states for capture by Ne^{2+}, transitions become possible at $R \leq 3.5$

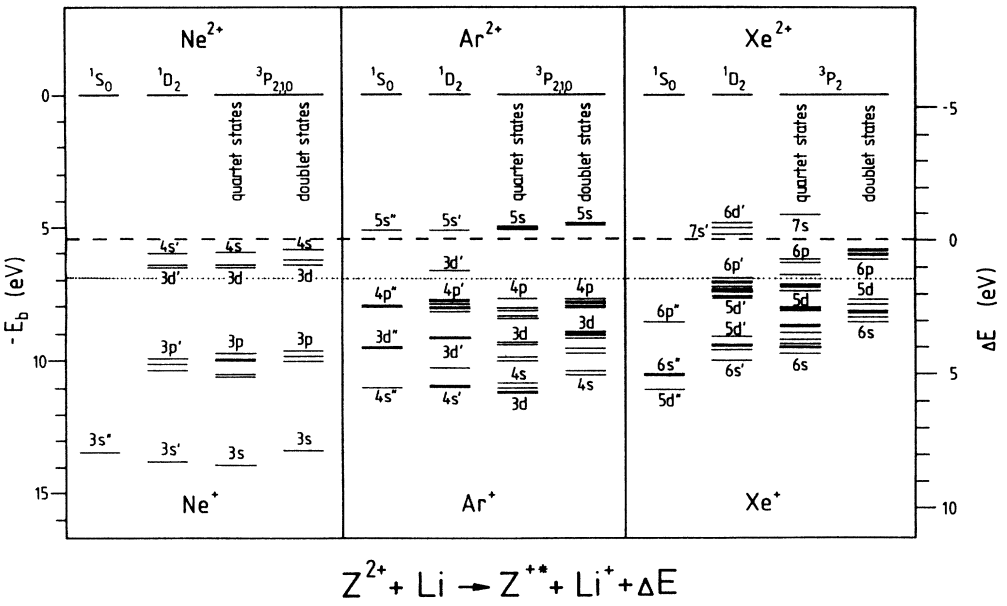

FIG. 4. Final projectile energy levels for electron capture from Li(2s) by Ne^{2+}, Ar^{2+}, and Xe^{2+}, respectively. The dashed line marks electron capture with reaction energy defect $\Delta E=0$, and the dotted line marks capture at the largest internuclear distance permitted by the CBM. For further explanations, see the text.

Å, resulting in $\sigma_{21} \leq 2\times10^{-15}$ cm^2. In the same way, for Ar^{2+} we find $R \leq 6.5$ Å and, consequently, $\sigma_{21} \leq 6.5\times10^{-15}$ cm^2. Such values are indeed measured at the lowest respective impact energies, cf. Figs. 3(a) and 3(b). On the other hand, for Xe^{2+} (and also for Kr^{2+}, where the pattern of final states is similar and therefore has not been shown in Fig. 4) an electron can be transferred at internuclear distances of almost R_c, at least for metastable primary ions. From this fact, the considerably larger σ_{21} values for Xe^{2+} and Kr^{2+} can be well understood. Finally, for N^{2+} the values obtained for σ_{21} can also be understood from the corresponding diagram of final states, which has been given in Fig. 7 of Ref. 2.

As expected, we found no dependence of σ_{21} on ion-source operating conditions, although we ensured production of ion beams with considerably different metastable fractions during different experimental runs, cf. Refs. 17 and 18.

D. Qualitative explanation of impact-energy dependence

The CBM can principally not explain the dependence of capture cross sections on impact energy. We will now give qualitative explanations for the experimentally determined impact-energy dependences shown in Figs. 3(a) and 3(b). The CBM assumes quasistatic approximation of the collision partners and therefore an equal chance of the electron to stick at the target or at the projectile.

The model, however, does not involve a variation of the transition probability or the internuclear location of the transition. Alternatively, the electron capture may be viewed as a transition between diabatic quasimolecular states of the colliding particles, cf. Ref. 1. In that picture, electronic transitions occur at crossings of potential-energy curves describing the quasimolecular states, with the transition probabilities depending on both the location of the crossings and the relative velocity of colliding particles.

Regarding the simplest case of two-state coupling, the transition probability passes its maximum at a relative velocity which is higher the smaller the crossing distance [or the larger the energy defect ΔE; cf. Eq. (5)]. The crossing distance, however, determines the electron-capture cross section because of geometrical reasons. Taking both influences together, the existence of a so-called "reaction window"[1] for electron capture by multicharged ions can be understood as the preference of final states with optimum energy defect ΔE resulting from the above considerations. The location of curve crossings within the reaction window apparently agrees with the transition distance as predicted by the CBM. However, if there are no final states fitting into the reaction window (as for capture by both Ne^{2+} and Ar^{2+}, cf. Fig. 4), the above-described quasimolecular model of electron capture can explain the impact-energy dependence of resulting total cross sections.

In the present range of impact velocity, coupling into final states inside the optimum internuclear distance (i.e., for Ne^{2+} into Ne^+ $3p$, for Ar^{2+} into Ar^+ $3d$ and $4p$; cf. Fig. 4) improves with rising impact velocity, which results in a corresponding behavior of total capture cross sections; cf. Fig. 3(a). In addition, for low primary ion charge state and only slightly exothermic reactions (i.e., small ΔE), the potential-energy curves intersect each other under small angles, which gives rise to an additional nonlocalized coupling inside the crossing distance, which also improves with increasing impact velocity. For capture by Ne^{2+}, the Ne^+ $3d$ states are available for such nonlocalized couplings[14] and thus contribute to the respective total electron capture; see Figs. 3(a) and 4. In

contrast to Ne^{2+} and Ar^{2+}, for both Kr^{2+} and Xe^{2+} a number of final states lies inside the reaction window; cf. Fig. 4. The efficiency of coupling into these states might slightly decrease with increasing impact velocity, and cannot be sufficiently counteracted by nonlocalized coupling into less tightly bound states.

The case of N^{2+} may be regarded as an intermediate one. However, a sounder explanation of impact-energy dependences calls for quantum-mechanical calculations, which so far have only been performed for He^{2+}-Li (see references given by Dijkkamp *et al.*[13]) and C^{4+}-Li collisions.[19]

IV. CONCLUSIONS

Total single-electron capture cross sections have been measured for impact of (5–40)-keV N^{2+}, Ne^{2+}, Ar^{2+}, Kr^{2+}, and Xe^{2+}, respectively, on Li($2s$). These measurements cover a range of impact velocities between 0.04 and 0.34 a.u., where a classical description of the capture process within the CBM should still be justified. Indeed, our results can be successfully explained in the CBM framework, if core conservation is assumed for the different primary-ion-beam components, and the actual structure of final projectile energy levels is taken into account. In this way it can also be explained why no influence on varying metastable admixture in the primary ion beam has been found.

Finally, invoking the quasimolecular description of electron capture and the impact-velocity dependence of involved potential-energy-curve crossings, an at least qualitative explanation of the remarkably different impact-energy dependences of the various total capture cross sections has been given.

ACKNOWLEDGMENTS

This work has been supported by Fonds zur Förderung der wissenschaftlichen Forschung (Projekt Nr. 5317) and by Kommission zur Koordination der Kernfusionsforschung at the Austrian Academy of Sciences.

[1]R. K. Janev and H. Winter, Phys. Rep. **117**, 265 (1985).
[2]A. Brazuk, D. Dijkkamp, A. G. Drentje, F. J. de Heer, and H. Winter, J. Phys. B **17**, 2489 (1984).
[3]D. Dijkkamp, A. Brazuk, A. G. Drentje, F. J. de Heer, and H. Winter, J. Phys. B **17**, 4371 (1984).
[4]H. Winter, Comments At. Mol. Phys. **12**, 165 (1982).
[5]F. Aumayr, M. Fehringer, and H. Winter, J. Phys. B **17**, 4185 (1984).
[6]F. Aumayr, M. Fehringer, and H. Winter, J. Phys. B **17**, 4201 (1984).
[7]F. Aumayr and H. Winter, Phys. Rev. A **31**, 67 (1985).
[8]F. Aumayr, G. Lakits, W. Husinsky, and H. Winter, J. Phys. B **18**, 2493 (1985).
[9]S. L. Varghese, W. Waggoner, and C. L. Cocke, Phys. Rev. A **29**, 2493 (1984).
[10]A. Brazuk, H. Winter, D. Dijkkamp, A. Boellaard, F. J. de Heer, and A. G. Drentje, Phys. Lett. **101A**, 139 (1984).
[11]W. Waggoner, C. L. Cocke, S. L. Varghese, and M. Stöckli, Phys. Rev. A **29**, 2457 (1984).
[12]R. W. McCullough, T. V. Goffe, M. B. Shah, M. Lennon, and H. B. Gilbody, J. Phys. B **15**, 111 (1982); G. A. Murray, J. Stone, M. Mayo, and T. J. Morgan, Phys. Rev. A **25**, 1805 (1982).
[13]J. L. Barrett and J. L. Leventhal, Phys. Rev. A **23**, 485 (1981); K. Kadota, D. Dijkkamp, R. L. van der Woude, A. de Boer, G. Y. Pan, and F. J. de Heer, J. Phys. B **15**, 3275 (1982); D. Dijkkamp, A. Boellaard, and F. J. de Heer, Nucl. Instrum. Methods B **9**, 377 (1985).
[14]E. Rille and H. Winter, J. Phys. B **15**, 3489 (1982).
[15]H. Ryufuku, K. Sasaki, and T. Watanabe, Phys. Rev. A **21**, 745 (1980).
[16]R. Mann, F. Folkmann, and H. F. Beyer, J. Phys. B **14**, 1161 (1981).
[17]F. Aumayr, G. Lakits, and H. Winter (unpublished).
[18]A. Brazuk and H. Winter, J. Phys. B **15**, 2233 (1982).
[19]W. Fritsch and C. D. Lin, J. Phys. B **17**, 3271 (1984).

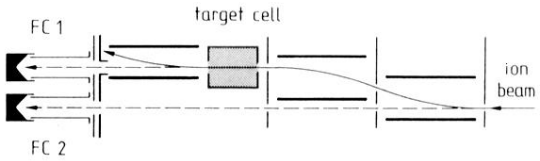

FIG. 1. Sketch of experimental setup with two parallel-plate condenser fields for ion-beam cleaning, Li-vapor target cell, charge-state-separation field, and Faraday cups. FC2 served for monitoring primary-ion-beam stability.